Journal of The Electrochemical Society, **147** (5) 1878-1881 (2000)
S0013-4651(99)11-087-5 CCC: $7.00

Influence of Geometry on the Electrochemical Response of Carbon Interdigitated Microelectrodes

Robert Kostecki,*,z Xiang Yun Song, and Kim Kinoshita*

Environmental Energy Technologies Division, Lawrence Berkeley National Laboratory, Berkeley, California 94720, USA

Microelectrodes were fabricated by carbonizing photoresist (700-1000°C) that was patterned on a Si wafer by use of a mask and UV photolithography. Two geometric designs of interdigitated carbon microelectrodes were produced with dimensions of about 500 μm length and 50 μm width. The carbon structures were characterized by Raman spectroscopy, atomic force microscopy, and optical microscopy. The electrochemical response of the microelectrodes was investigated by cyclic voltammetry using the I_3^-/I^- redox couple. The collection efficiencies of carbon interdigitated array electrodes (IDAEs) varied from 59 to 90% depending on the cell size, geometry, and generator-collector arrangement. These collection efficiencies are comparable to those reported with multiband ($n > 25$ bands) IDAEs.

Manuscript submitted November 24, 1999; revised manuscript received January 19, 2000.

Electrodes of small dimensions, commonly referred to as microelectrodes, are attracting attention for applications that include sensors, detectors and microelectromechanical systems (MEMS).[1-3] These electrodes are fabricated in a variety of structures, different geometric arrangements, and of different compositions. Semiconductor processing techniques that involve photolithography, reactive ion etching, vapor deposition, etc. are suitable methods for fabricating microelectrodes. Dimensions of <10 μm for the width and separation of microelectrodes are feasible by these techniques.

Microelectrodes are being actively considered for electrochemical applications.[4,5] In particular, microelectrodes have attracted attention for use in chemical analysis.[6-13] Both two-dimensional microdisk[6,9,10,13,14-16] and one-dimensional band[7,8,17-19] electrodes are under investigation. An advantage of these microelectrode systems is the sensitivity to detection of low concentrations of electroactive species.

Microelectrodes exhibit a different electrochemical response to redox species in solution than large planar electrodes. Cyclic voltammetry of redox species at large planar electrodes shows current-potential profiles that are indicative of current peaks during the anodic and cathodic potential sweeps. On the other hand, cyclic voltammetry of microelectrodes reveals the presence of a current plateau rather than a current peak when the redox species undergoes electrochemical reaction. Because of their small dimensions, spherical diffusion occurs at the microelectrodes rather than linear diffusion.

The use of photolithography and patterned photoresists offer an interesting option for design and fabrication of different electrode structures of microdimensions. Kostecki *et al*.[20] demonstrated the electrochemical behavior of carbon interdigitated array electrodes (IDAEs) fabricated from carbonizing photoresist that was spin coated on an Si wafer and patterned in an array by photolithography. Extension of the electrochemical studies of carbon IDAEs is the subject of this paper, and in particular, we report results obtained with carbon films produced from different photoresists pyrolized at 700 and 1000°C and with another carbon IDAE array of different geometry.

Experimental

The processing steps that were used to fabricate the carbon IDAEs are described in detail elsewhere.[20] Positive photoresists, AZ-4330 (Hoechst Celanese) and S1818 (Shipley), were used as the precursor in this study to produce the carbon electrodes. The procedure that was used to fabricate the carbon IDAEs consisted of a sequence of processing steps that are typically used in the semiconductor industry. The photoresist was spin coated on a 10 cm Si wafer that had a thin (~100 nm) Si_3N_4 layer which served as an insulating substrate on which the carbon structure was formed. Two masks were designed and used with ultraviolet (UV) photolithography to form the interdigitated structures. After the appropriate processing steps (*i.e.*, baking and developing), the wafers with the patterned photoresist were heat treated at 700-1000°C in an inert environment to form the carbon IDAEs.

Figure 1 shows a schematic representation of the two IDAE arrays that depict the single-cell (A) and double-cell (B) geometry. In the single-cell geometry, the two electrodes have the same area. With the double-cell geometry, one electrode has a larger area than the other, and furthermore it essentially "surrounds" the other electrode. This arrangement is more similar than the single-cell geometry to the configuration of the ring-disk electrode. The nominal dimensions for the interdigitated structures studied in this work are presented in Table I. The surface profile of the single-cell geometry was presented elsewhere.[20] The analysis showed that the carbon digits in the interdigitated structure have an irregular profile, with the cross section having a cone shape.

The dimensions of the carbon IDAEs are dependent on the design and pattern on the photomask because contact printing was used. The patterns were designed to include fingers as small as 5 μm width to as large as 52 μm width and separated by 5 or 10 μm. After carbonization, however, a noticeable shrinkage in the dimensions is evident. Because of technical difficulties encountered so far in fabricating the small dimensions, only results obtained with the larger carbon IDAEs are presented here.

Various techniques including Raman spectroscopy (RS), atomic force microscopy (AFM) and optical microscopy were used to examine the structure of the carbon. Raman spectroscopy measurements were carried out at room temperature in ambient atmosphere using an argon ion laser (Coherent Inc., model Innova 70) tuned to 514.5 nm. The details on Raman spectroscopic studies of carbon using this instrument were presented earlier.[21] A surface profile analyzer (NewView System 200, Zygo Corp., Middlefield, CT) that combines optical microscopy and interferometry was used to obtain images of the microstructure and 3-D surface topography. *Ex situ* AFM images were obtained with a molecular imaging (MI) scanning probe microscope coupled with a Park Scientific Instruments (PSI) electronic controller. For the AFM measurements PSI MLCT-AUNM microcantilevers (0.05 N m^{-1}) were used. A four-point probe was used to determine the electrical resistance of the carbon films.

The I_3^-/I^- redox couple was used to investigate the electrochemical properties of the carbon IDAEs. Reagent-grade chemicals and double distilled water was used to prepare 0.1 M KI and 0.1 M H_2SO_4 solutions. Details on the cell design and electrode connections are described by Kostecki *et al.*[20] A bipotentiostat (model RDE4, Pine Instrument Company) was used for the electrochemical

* Electrochemical Society Active Member.
z E-mail: r_kostecki@lbl.gov

S0013-4651(99)11-087-5 CCC: $7.00

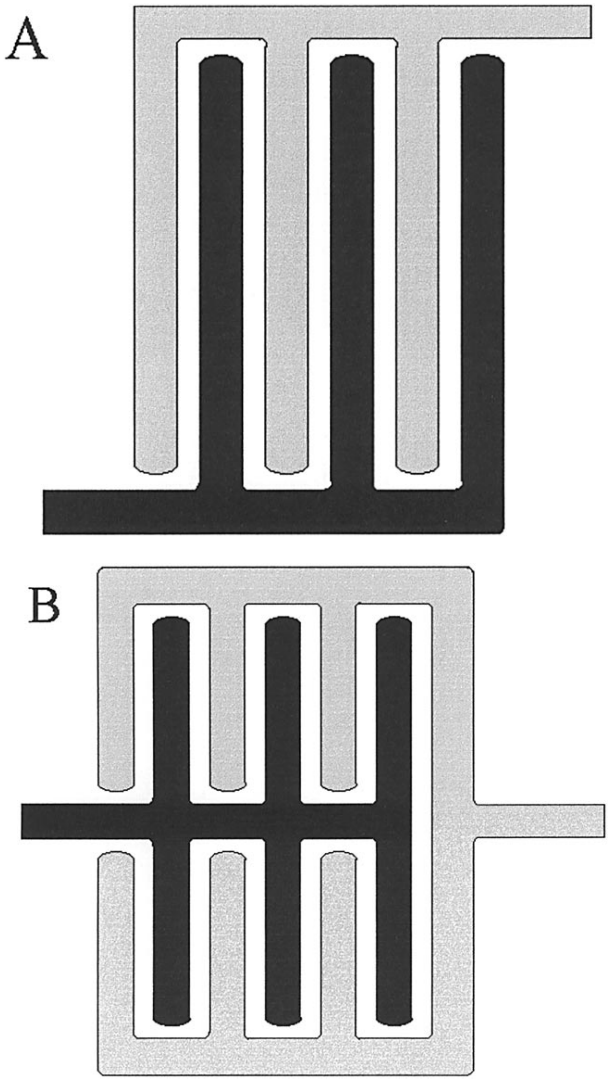

Figure 1. Schematic representation of the two IDAE arrays: (A) single cell geometry, (B) double-cell geometry.

measurements. All potentials were measured with respect to a Ag/AgCl/KCl (sat.) reference electrode.

Results

The AFM images of the carbon thin-film electrode reveal a compact surface structure.[6] The surface appears to be relatively smooth and uniform, and free of cracks and large aggregates (Fig. 2). This structure was typical for all carbon films heat treated at 700-1000°C in inert atmosphere. Statistical analysis of this featureless surface reveals a peak-to-valley distance of ~12 Å and an rms roughness of ~1.7 Å. The thickness of the carbon film was determined to be 2 μm. The films heat-treated at temperatures ≤1000°C do not exhibit large crystallites or graphite-type planes and steps. Instead, they

Table I. Characteristics of carbon IDAEs.

Sample type	Dimensions (μm)	Finger width (μm)	Finger gap (μm)
1A symmetric	250 × 400	33	7.5
2A symmetric	370 × 600	52	12
1B asymmetric	290 × 440	33	9.4
2B asymmetric	430 × 660	52	9.4

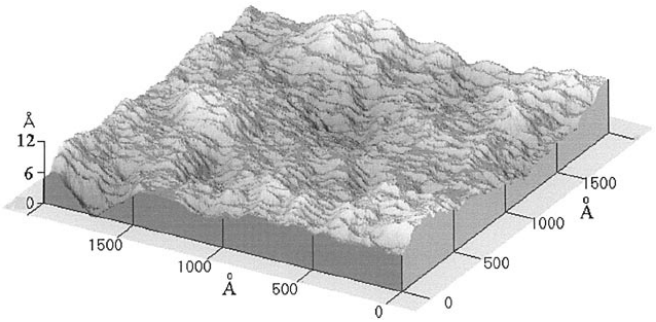

Figure 2. AFM image of the carbon thin film electrode produced from Shipley 1818 photoresist pyrolyzed at 1000°C.

consist of small 2.0-3.0 nm crystallites distributed in the predominantly amorphous material.[22]

Figure 3 shows the first-order Raman spectra for carbonaceous films produced at two different temperatures. Both spectra show a strong and broad D-band at 1350 cm^{-1} with a broad G-graphite band shifted toward higher frequencies (~1600 cm^{-1}). The spectra of the carbon films represent the general behavior of vibrational spectra obtained from highly disordered carbonaceous materials. Surprisingly, the intensity of the G-band is higher for the carbon film heat-treated at 700°C compared to that produced at 1000°C. In fact, the band at 1600 cm^{-1} has a doublet structure and consists of the characteristic graphite E_{2g} band located at 1576 cm^{-1} and another band at 1620 cm^{-1}. The observed effect is associated with the intensity variation of the Raman peak at 1620 cm^{-1}. In fact, the intensity of this band is directly related to the degree of disorder of carbonaceous materials and to the amount of crystal boundary. Thus, one can expect that this band contributes significantly to the broad peak at 1600 cm^{-1}, which is also observed in the spectra of carbon films heat-treated at lower temperatures.

The electrochemical properties and stability of the carbon films were investigated by cyclic voltammetry at scan speed of 50 mV/s in 0.1 M H_2SO_4 solution. Figure 4 shows cyclic voltammograms (CVs) of two 2B-type IDAEs (see Table I for details) fabricated from Shipley S1818 and AZ4330 positive photoresists by pyrolysis at 1000 and 700°C, respectively. Each of the carbon films displays different electrochemical behavior. The film produced at 700°C

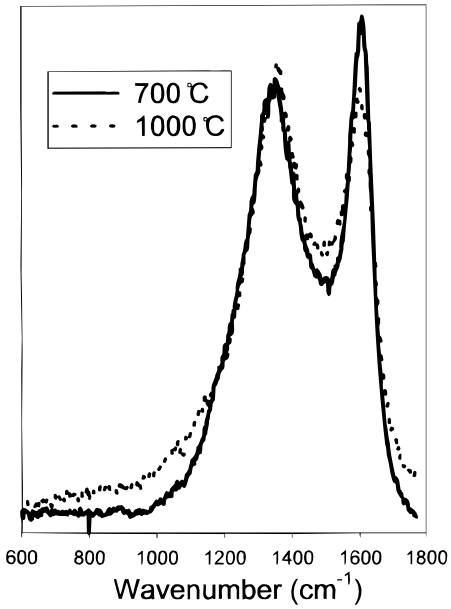

Figure 3. Raman spectra of carbonaceous films produced from AZ4330 and Shipley 1818 positive photoresists pyrolyzed at 700 and 1000°C, respectively.

S0013-4651(99)11-087-5 CCC: $7.00

shows very little electrochemical activity in the cathodic region and almost no activity in the anodic potential range. However, the current-potential profile changes dramatically for the carbon film obtained as the pyrolysis temperature is increased from 700 to 1000°C. This carbon electrode shows no significant electrochemical reactions between 0.5 and 1.2 V, and the potential range is limited by oxygen reduction and oxygen evolution, respectively. A contribution from redox surface groups is also visible (redox couple at −0.05 V). The surface electrical resistivity of the carbon films produced at 700°C was two orders of magnitude higher than the carbon films pyrolized at 1000°C. This change in the film resistance is believed to be due to changes in the film composition, for example, the H/C ratio.[22] Lack of electrochemical activity of the carbon electrodes heat-treated at 700°C made them unusable for electroanalytical studies, and therefore, we focused exclusively on the carbon IDAEs pyrolyzed at 1000°C.

The I_3^-/I^- redox couple, which provides a highly sensitive electrochemical response to electrode surfaces, was used to investigate the electrocatalytic properties of the carbon IDAEs. The electrochemical response of the 2A symmetric carbon IDAE is illustrated by the CV (scan rate 100 mV/s) and the amperogram presented in Fig. 5. Both of the carbon IDAEs (later referred to as the generator and collector electrodes) were operated in the potentiostatic mode in this case. The potential of the collector electrode was kept constant at −0.1 V while a linear potential sweep (100 mV/s) between −0.7 and 0.42 V was applied to the generator electrode. The current deected at these electrodes during the voltammetric sweep is expressed *vs.* the potential of the generator electrode. In this experiment, I_3^- ions that are produced at the generator electrode are detected at the collector electrode which is set at a potential where I_3^- is reduced to I^- ions according to Reaction 1

$$I_3^- + 2e^- \leftrightarrow 3I^- \qquad [1]$$

During the anodic potential scan of the generator electrode, I^- ions are oxidized to I_3^- at potentials higher than 0.3 V. Their presence is detected at the cathodically polarized collector electrode where the I_3^- ions produced at the generator electrode are reduced back to I^-. At potentials lower than about −0.4 V, hydrogen evolution starts to contribute to the cathodic current at the generator electrode.

The close proximity of the two IDAEs provides a convenient arrangement to evaluate their viability as a substitute for a ring-disc electrode. In order to evaluate quantitatively the collection coefficient of the IDAEs of different sizes and geometries a series of

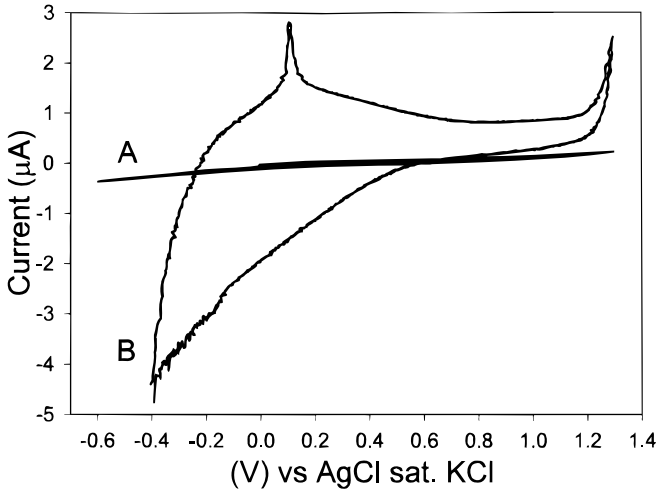

Figure 4. CVs of a double geometry 2B cell (both electrodes short-circuited) fabricated from AZ4330 (A) and Shipley 1818 (B) positive photoresists pyrolyzed at 700 and 1000°C, respectively. Potential scans were carried out at 50 mV/s in 0.1 M H_2SO_4 solution.

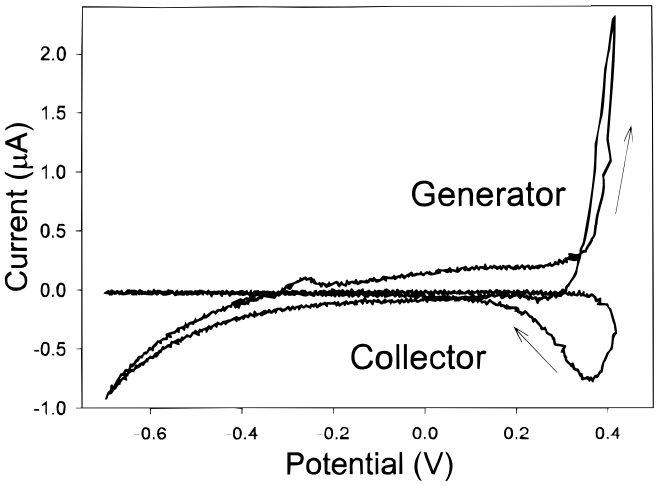

Figure 5. Electrochemical response of the 2A single geometry cell in 0.1 M KI. One electrode (generator) was scanned at 100 mV/s while the other one (collector) was held at constant potential of −0.1 V.

amperometric measurements were carried out. In this case, the rate of the anodic reaction at the generator electrode was controlled galvanostatically. A slow 10 nA/s current scan from 0 to 5.9 μA was implemented on the generator electrode to produce I_3^- ions that were reduced back to I^- at the collector electrode which was polarized potentiostatically at −0.1 V. The results obtained for the iodine system with the present microelectrode geometry are shown in Fig. 6. The increase in the anodic current at the generator electrode during the scan produces a cathodic current response of a similar magnitude at the collector electrode. The cathodic current at the collection electrode shows a slight hysteresis with a higher current observed during the reverse potential scan on the generator electrode. The contribution from I_3^- ions that escaped and accumulated in the electrolyte during the anodic scan is responsible for this behavior. The generator-collector relationship shows very good linearity within 0-5 μA current range, and the collection efficiency can be easily determined from the slope of the current line.

The collection efficiency of the symmetric IDAEs was practically identical for both, the 1A and 2A size cells (Fig. 6A), and reached 71%. The double geometry IDAE cells, 1B and 2B, exhibited current asymmetry, depending on the generator-collector configuration. In the optimal configuration, *i.e.*, 2B IDAEs, with the inner electrode as a generator, the collection efficiency reached almost 90%. It dropped for obvious geometric reasons to 69% when the generator-collector configuration was reversed. Interestingly, the collection efficiencies calculated from the results in Fig. 6C, *i.e.*, for smaller size asymmetric IDAEs, are substantially lower than for larger cells and are 69 and 59% for inner and outer generator configuration, respectively. Surprisingly, it is lower than the efficiency measured with the less favorable symmetric design.

Aoki *et al.*[23] reported that the collection efficiency based on steady-state currents is *ca.* 90-100% at an metallic (Pt) interdigitated array electrodes (IDAEs) in a stationary solution. They found that the collection efficiency at the microband electrode configuration *i.e.*, alternative band array structure($n > 25$ bands), is only influenced by geometrical factors and varies by changing not only the gap but also the bandwidth.

The observed collector-electrode currents directly reveal the diffusion characteristics between the generator and collector electrodes. For the single geometry cell the collection efficiency does not vary with the cell size because the bandwidth-to-gap ratio remains almost the same. In the double-geometry cell, the collection efficiency can reach values close to those reported for IDAEs and the reason for the observed decrease in the cell efficiency is related to the proportionally larger gap between the fingers in the smaller cell. However, the collection coefficients for all geometrical configurations studied in this

S0013-4651(99)11-087-5 CCC: $7.00

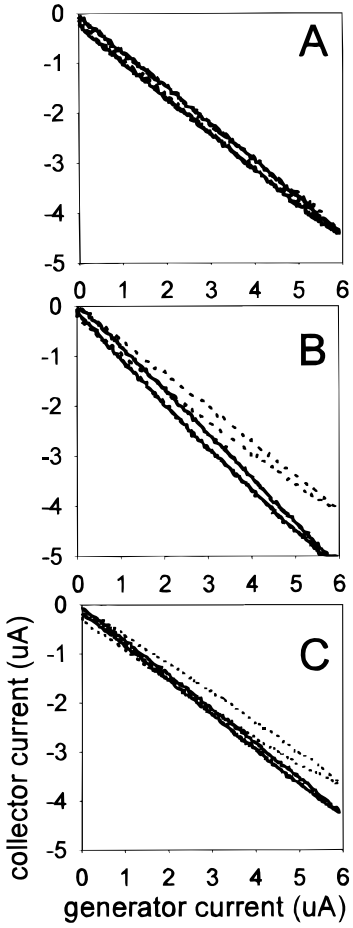

Figure 6. Electrochemical response of the 1A, 2A single-geometry cells (A), 2B and 1B double-geometry cells (B), (C) respectively. Solid line: inner electrode as a generator. Dotted line: outer electrode as a generator. Slow 10 nA/s current scan from 0 to 5.9 μA was implemented on the generator. Collector electrode was held at −0.1 V.

work exceed those typically observed with rotating ring-disk electrodes (0.2-0.4). Moreover, the asymmetric geometry of IDAE can help reduce the "feedback effect" usually associated with IDAEs.

Conclusions

The initial results presented here illustrate the electrochemical response of the pyrolytic carbon IDAEs to redox reactions, and demonstrated that by varying the geometric arrangement of IDAEs, collection efficiencies comparable to multiband IDAEs can be obtained. This study demonstartes that semiconducor-processing techniques are a promising and viable approach to producing carbon microelectrode for miniaturized electrochemical systems.

Acknowledgment

This work was supported by the Director, Office of Energy Research, Office of Basic Energy Sciences, Chemical Sciences Division of the U.S. Department of Energy under contract no. DE-AC03-76SF00098.

Lawrence Berkeley National Laboratory assisted in meeting the publication costs of this article.

References

1. P. Tomcik, S. Mesaros, and D. Bustin, *Anal. Chim.*, **374**, 283 (1998).
2. O. Niwa and H. Tabei, *Anal. Chem.*, **66**, 285 (1994).
3. M. Shibuya, T. Nishina, T. Matsue, and I. Uchida, *J. Electrochem. Soc.*, **143**, 3157 (1996).
4. C. R. Martin and D. T. Mitchell, in *Electroanalytical Chemistry*, Vol. 21, A. J. Bard and I. Rubinstein, Editors, p. 1, Marcel Dekker, New York (1999).
5. M. Nishizawa and I. Uchida, *Electrochim. Acta*, **44**, 3629 (1999).
6. D. A. Fungaro and C. M. A. Brett, *Anal. Chim. Acta*, **385**, 257 (1999).
7. Z. M. Liu, J. Li, T. Y. You, X. R. Yang, and E. K. Wang, *Electroanalysis*, **11**, 53 (1999).
8. F. M. Matysik, F. Bjorefors, and L. Nyholm, *Anal. Chim. Acta*, **385**, 409 (1999).
9. C. J. Slevin, N. J. Gray, J. V. Macpherson, M. A. Webb, and P. R. Unwin, *Electrochem. Commun.*, **1**, 282 (1999).
10. T. G. Strein, B. J. Ximba, and A. H. Hamad, *Electroanalysis*, **11**, 37 (1999).
11. A. Vogel and J. W. Schultze, *Electrochim. Acta*, **44**, 3751 (1999).
12. T. Y. You, X. R. Yang, and E. K. Wang, *Electroanalysis*, **11**, 459 (1999).
13. Y. D. Zou and J. Y. Mo, *Anal. Chim. Acta*, **382**, 145 (1999).
14. J. E. Baur, H. M. Miller, and M. A. Ritchason, *Anal. Chim. Acta*, **397**, 123 (1999).
15. C. S. Henry and I. Fritsch, *Anal. Chem.*, **71**, 550 (1999).
16. R. S. Rashkov, R. Aogaki, and S. Nakabayashi, *Chem. Lett.*, **1**, 97 (1999).
17. M. Nishizawa and I. Uchida, *Electrochemistry*, **67**, 420 (1999).
18. E. W. H. Jager, E. Smela, and O. Inganas, *Sens. Actuators B, Chem.*, **56**, 73 (1999).
19. T. Makela, S. Pienimaa, S. Jussila, and H. Isotalo, *Synth. Met.*, **101**, 705 (1999).
20. R. Kostecki, X. Song, and K. Kinoshita, *Electrochem. Solid-State Lett.*, **2**, 461 (1999).
21. R. Kostecki, T. Tran, X. Y. Song, K. Kinoshita, and F. McLarnon, *J. Electrochem. Soc.*, **144**, 3111 (1997).
22. J. Kim, X. Song, K. Kinoshita, M. Madou, and R. White, *J. Electrochem. Soc.*, **145**, 2314 (1998).
23. K. Aoki, M. Morita, O. Niwa, and H. Tabei, *J. Electroanal. Chem. Interfacial Electrochem.*, **256**, 269 (1988).